PAPER

Check for updates

Bio-guided isolation of alpha-glucosidase inhibitory compounds from Vietnamese liverwort *Marchantia polymorpha*: *in vitro* and *in silico* studies†

Ngoc Khanh Van Nguyen ,[a] Ho-Duc-Trung Tran,[b] Thuc-Huy Duong,[b] Nguyen Kim Tuyen Pham,[c] Thi Quynh Trang Nguyen,[c] Thi Ngoc Thao Nguyen,[c] Warinthorn Chavasiri,[de] Ngoc-Hong Nguyen*[f] and Huu Tri Nguyen [ID] *[a]

Bio-guided isolation was applied to Vietnamese *Marchantia polymorpha* L. to find alpha-glucosidase inhibition. Fifteen compounds were isolated and structurally determined, including two new compounds, marchatoside (**7**) and marchanol (**8**), along with thirteen known compounds: marchantin A (**1**), isoriccardin C (**2**), riccardin C (**3**), marchantin K (**4**), lunularin (**5**), 3R-(3,4-dimethoxybenzyl)-5,7-dimethoxyphthalide (**6**), vitexilactone (**9**), 12-oleanene-3-one (**10**), 3,11-dioxoursolic acid (**11**), ursolic acid (**12**), artemetin (**13**), kaempferol (**14**), and quercetin (**15**). The structures of these compounds were determined through extensive spectroscopic analyses (1D and 2D NMR, HRESIMS, and ECD) and by comparisons to the existing literature. There are five types of carbon skeleton, including bibenzyl (**1–5**), 3-benzylphthalide (**6** and **7**), diterpenoid (**8** and **9**), triterpenoid (**10–12**), and flavonoid (**13–15**). Compounds **6–12** were reported for the first time within the genus *Marchantia*. Compounds **1–12** were evaluated for their alpha-glucosidase inhibition. Among them, **1–5** and **10–12** displayed potent inhibition, with IC_{50} values ranging from 28.9 to 130.6 μM, compared to the positive control acarbose 330.9 μM. A kinetic study and molecular docking were also performed to understand the mechanism.

1. Introduction

Marchantia polymorpha L. is a liverwort belonging to the family Marchantiaceae, widely distributed in mountainous regions.[1] It is believed to be a valuable source of traditional medicines in India, China, Europe, and Vietnam.[1,2] In folk medicine, it has been used to treat inflammation, liver disease, wounds, boils, insect bites, and snake bites.[1] Chemical data of this liverwort have been comprehensively investigated, indicating the presence of over 50 compounds (Fig. S1†).[3–10] Among these compounds, 11 known components were found in the native

liverwort in Vietnam (Fig. S2†).[11,12] The major carbon skeletons of these compounds were found to be bis-bibenzyls, sesquiterpenoids, flavonoids, phenolics, coumarins, and glycosides. The extracts of this liverwort showed antioxidant and antibacterial properties, inhibition of tyrosinase and alpha-glucosidase, as well as cytotoxicity against several cancer cell lines.[13–18] However, little is known about the alpha-glucosidase inhibitors from this medicinal source, with only two reports.[17,18] These authors conducted the biological evaluation of extracts derived from natural and cultured *M. polymorpha*, indicating the potent inhibition of all prepared extracts. Bio-guided isolation was applied to Vietnamese *M. polymorpha* to find alpha-glucosidase inhibition. Fifteen compounds were isolated (Fig. 1). The structures of these compounds were determined through extensive spectroscopic analyses (1D and 2D NMR, HRESIMS, and ECD). Two new compounds, marchatoside (**7**) and marchanol (**8**), together with thirteen known compounds, marchantin A (**1**), isoriccardin C (**2**), riccardin C (**3**), marchantin K (**4**), lunularin (**5**), 3R-(3,4-dimethoxybenzyl)-5,7-dimethoxyphthalide (**6**), vitexilactone (**9**), 12-oleanene-3-one (**10**), 3,11-dioxoursolic acid (**11**), ursolic acid (**12**), artemetin (**13**), kaempferol (**14**), and quercetin (**15**) were structurally determined. A brominated derivative **1a** of marchantin A was prepared. All compounds

[a]*Faculty of Natural Sciences Pedagogy, Sai Gon University, 273 An Duong Vuong, Ward 3, District 5, Ho Chi Minh City 70000, Vietnam. E-mail: trihuunguyen@sgu.edu.vn*

[b]*Department of Chemistry, Ho Chi Minh City University of Education, 280 An Duong Vuong Street, District 5, Ho Chi Minh City 748342, Vietnam*

[c]*Faculty of Environment, Sai Gon University, 273 An Duong Vuong, Ward 3, District 5, Ho Chi Minh City 70000, Vietnam*

[d]*Center of Excellence in Natural Products Chemistry, Department of Chemistry, Faculty of Science, Chulalongkorn University, Pathumwan, Bangkok, 10330, Thailand*

[e]*Nanotec-CU Center of Excellence on Food and Agriculture, Department of Chemistry, Faculty of Science, Chulalongkorn University, Bangkok, 10330, Thailand*

[f]*CirTech Institute, HUTECH University, 475 A Dien Bien Phu Street, Binh Thanh District, Ho Chi Minh City, Vietnam. E-mail: nn.hong@hutech.edu.vn*
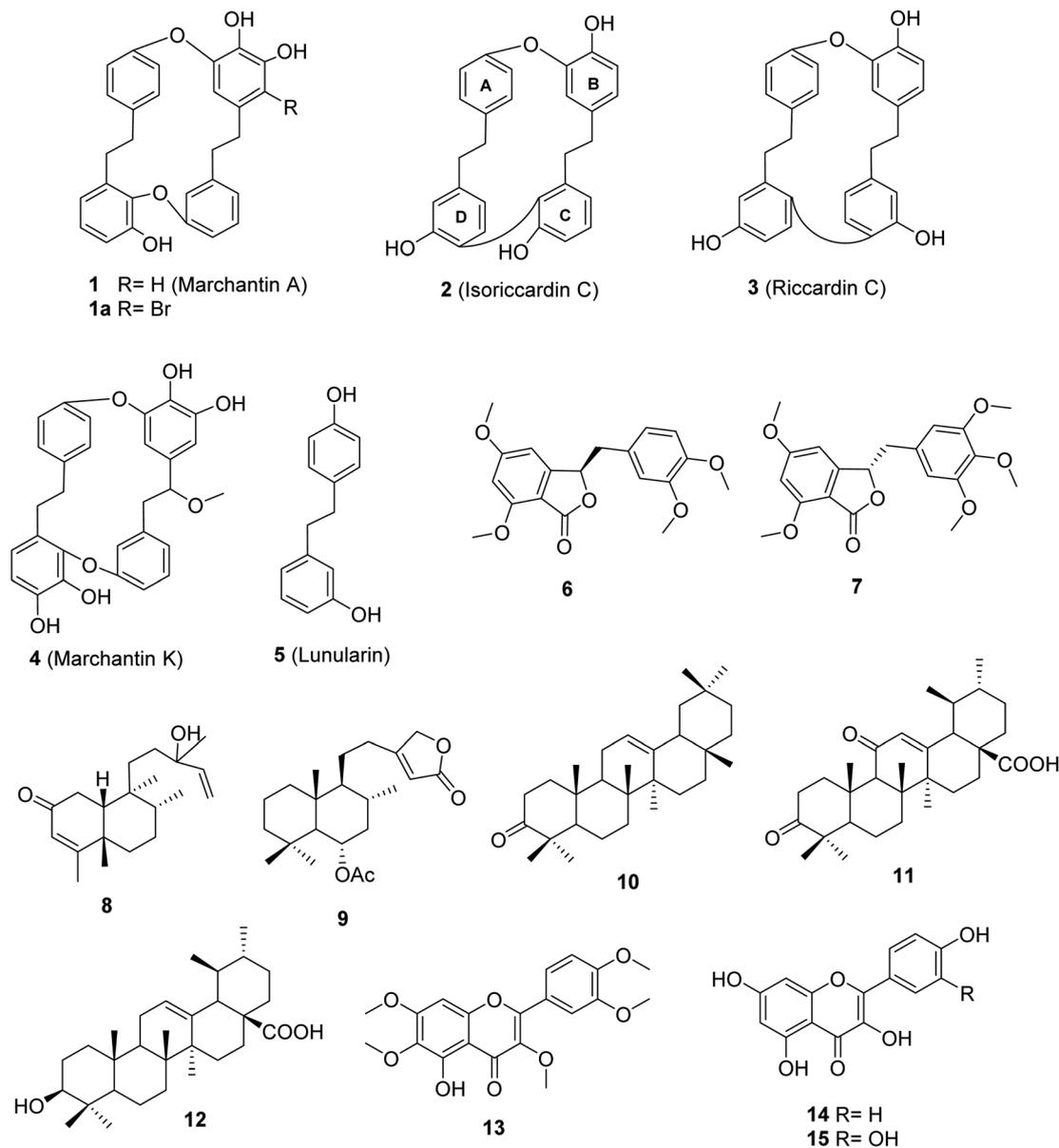
Fig. 1 Chemical structures of **1–15**.

were evaluated for their alpha-glucosidase inhibition. A kinetic study and molecular docking were also performed to understand the mechanism.

2. Results and discussion

The crude extract of *M. polymorpha* was prepared using EtOAc. This crude extract was evaluated for alpha glucosidase inhibition, indicating moderate activity with an IC$_{50}$ value of 27.7 ± 1.2 µg mL^{-1}. The solvent ethyl acetate was selected for maceration based on the results reported by Tran *et al.* (2018).[16] These authors prepared four *n*-hexane, chloroform, ethyl acetate, and ethanol extracts from natural *M. polymorpha* and evaluated their alpha-glucosidase inhibition. The ethyl acetate extract showed the strongest activity, with an IC$_{50}$ value of 10.3 µg mL^{-1}.[16] In 2020, this team also evaluated the inhibition of the cultured *M.*

polymorpha biomass,[17] indicating that *n*-hexane extract showed potent inhibition with an IC$_{50}$ value of 11.9 µg mL^{-1}.

Two new compounds, marchatoside (**7**) and marchanol (**8**), along with thirteen known compounds, marchantin A (**1**),[18] isoriccardin C (**2**),[4] riccardin C (**3**),[4,12] marchantin K (**4**),[19] lunularin (**5**),[12] 3*R*-(3,4-dimethoxybenzyl)-5,7-dimethoxyphthalide (**6**),[20] vitexilactone (**9**),[21] 12-oleanene-3-one (**10**),[22] 3,11-dioxoursolic acid (**11**),[23] ursolic acid (**12**),[24] artemetin (**13**),[25] kaempferol (**14**),[13] and quercetin (**15**)[12] were structurally determined. To the best of our knowledge, compounds **7–11** were reported for the first time in liverworts. Isolated compounds were classified as bis-bibenzyl (**1–4**), bibenzyl (**5**), 3-benzylphthalide (**6** and **7**), diterpene (**8** and **9**), triterpene (**10–12**), and flavanols (**13–15**). Many natural 3-benzylphthalide-type compounds have been reported, but little is known about their absolute configuration.[26–29] 3-Benzylphthalide-type compounds have not

been reported in the genus *Marchantia*, but they were found previously in *Frullania* sp. and *Porella perrottetiana* liverworts.[29] A few clerodane-type and *ent*-labdane-type diterpenoids were previously isolated in liverworts: *Gottschelia schizopleura*[30] and *Jamesoniella autumnalis*.[31] However, these types of compound were rarely found in liverworts. Compound **6** was previously isolated from the liverwort *Frullania muscicola*,[20] but the absolute configuration of C-3 was unknown. ECD data of **6** was recorded, showing a strong negative Cotton effect around 240–250 nm. This CE was consistent with that of julacelide reported in our previous paper,[32] proposing the absolute C-3 configuration as 3*R*. Comparison of NMR data of known compounds **1–6**, **8–11** with those reported in the literature gave consistency (see Tables S1–S12†). Compound **1** was selected for bromination in order to find a better alpha-glucosidase inhibitor. Electrophilic aromatic bromination was applied to **1**, yielding product **1a** (see Scheme S1†). The chemical structure of **1a** was defined using the spectroscopic method (see Table S13†). Unfortunately, compound **1a** showed weaker activity than the parent compound **1**, thus no further halogenated modifications were conducted on **1**.

Compound **7** was obtained as a colorless oil. The molecular formula of **7** was deduced as $C_{20}H_{22}O_7$ from the protonated molecular ion peak at *m/z* 375.1397 (calcd for $[C_{20}H_{22}O_7 + H]^+$, 375.14438) in the HRESI mass spectrum (Fig. S9A†). The ^{1}H NMR spectrum showed two aromatic protons of a symmetric 1,3,4,5-tetrasubstituted benzene ring (δ_H 6.58, s, H-2′ and H-6′), two meta-coupled aromatic protons [δ_H 6.59 (1H, d, *J* = 1.5, H-4) and 6.54 (1H, d, *J* = 1.5, H-6)], five methoxy groups [δ_H 3.88 (3H, s, 5-OCH₃), 3.87 (3H, s, 7-OCH₃), 3.75 (6H, s, 3′-OCH₃ and 5′-OCH₃), and 3.67 (3H, s, 4′-OCH₃)], and one oxygenated methine [δ_H 5.62 (1H, dd, *J* = 6.5, 5.5, H-3)] coupled with two protons of one methylene group [δ_H 3.25 (1H, dd, *J* = 14.5, 5.5, H-10a) and 3.10 (1H, dd, *J* = 14.0, 6.5, H-10b)]. The JMOD and HSQC spectra exhibited 20 carbon resonances attributable to a carboxyl ester group (δ_C 167.5), four aromatic methine carbons (δ_C 108.2 × 2, 99.7, and 99.4), one oxygenated methine carbon (δ_C 80.2), one methylene carbon (δ_C 41.4), five methoxy carbons (δ_C 60.5, 56.4, 56.4, 56.4, and 56.2), and eight quaternary carbons [δ_C 167.4, 160.4, 155.3, 154.1 (× 2), 137.2, 132.6, and 107.8]. The above spectroscopic data indicated that **1** was a 3-benzylphthalide derivative.[32] In the so-called A-ring, the protons at δ_H 6.59 (H-4) and δ_H 6.54 (H-6) gave HMBC correlations to the same carbons at δ_C 167.4 (C-5), 155.3 (C-9), and 107.8 (C-8)

indicated the connection through C-4 to C-9 (Fig. 2). The methoxy groups at δ_H 3.88 and 3.87 were determined to be located at C-5 and C-7 in this A-ring due to their HMBC correlations to these carbons. The methine group at δ_H 5.62 was coupled with the methylene CH₂-10 (δ_H 3.25 and 3.10) in an ABX system characteristic of 3-benzylphthalide derivatives.[25–28] Next, the methylene group H₂-10 gave HMBC correlations to carbons at δ_C 132.6 (C-1′) and 108.2 (C-2′ and C-6′), and 122.9 (C-6′) indicated the connectivity between A and B-rings through C-3 and C-10 (Fig. 2). The lactonization between C-1 and C-3 was defined by the HMBC correlation of H-3 to C-1 and the downfield chemical shift of H-3.[32] NMR data of **7** were similar to those of **6** (Table 1). The only difference is the occurrence of the methoxy group at C-3′. The absolute configuration of **7** was defined using ECD data. Particularly, a positive Cotton effect at 260 nm indicated the 3*S* configuration of **7** (Fig. 3). This CE was opposite that of julacelide isolated from the moss *Erythrodontium julaceum*. Combined, the chemical structure of **7** was elucidated as shown in Fig. 1, namely marchatoside.

Compound **8** was obtained as a colorless oil. The molecular formula of **8** was deduced as $C_{20}H_{32}O_2$ from the sodiated molecular ion peak at *m/z* 327.2295 (calcd for $[C_{20}H_{32}O_2 + Na]^+$, 327.2300) in the HRESI mass spectrum (Fig. S10A†). The ^{1}H NMR spectrum showed an olefinic proton (δ_H 5.56, d, *J* = 1.0, H-3), a vinyl group [δ_H 5.93 (1H, dd, *J* = 17.0, 1.5, H-14), 5.21 (1H, dd, *J* = 17.5, 2.0, H-15a), and 4.98 (1H, dd, *J* = 11.0, 2.0, H-15b)], five methyl groups [δ_H 1.96 (d, *J* = 1.0), 1.25, 1.24, 0.78 (d, *J* = 7.0), and 0.56], and an ABX system of a methylene [δ_H 2.66 (1H, dd, *J* = 18.5, 7.0, H-1a) and 2.43 (1H, d, *J* = 18.0, H-1b)] coupled with a methine [δ_H 1.90 (1H, m, H-10)]. The JMOD and HSQC spectra exhibited a ketone carbonyl group (δ_C 198.8), two olefinic methine carbons (δ_C 129.1 and 147.1), one olefinic methylene carbon (δ_C 111.5), one oxygenated quaternary carbon (δ_C 72.8), five methyl carbons (δ_C 32.3, 28.5, 20.5, 19.6, and 16.3), five methylene carbons (δ_C 37.5, 37.4, 35.8, 35.7, and 31.3), two sp³ methine (δ_C 47.9 and 37.4), and three quaternary carbons (δ_C 169.4, 40.3, and 40.1). The above spectroscopic data indicated that **1** was a clerodane diterpene.[33–36] HMBC correlations supported the chemical structure of **8** (Fig. 4). At first, the HMBC correlations of H₃-18 (δ_H 1.96) and H₃-19 (δ_H 1.25) to C-4 (δ_C 169.4) and C-5 (δ_C 40.1), of H-3 (δ_H 5.56) to C-4 and C-1 (δ_C 35.7), and of H₂-1 (δ_H 2.66 and 2.43) and H-10 (δ_H 1.99) to C-2 (δ_C 198.8) defined the structure of the A-ring (Fig. 4). Both methyl H₃-19 and H₃-20 (δ_H 0.56) gave a HMBC correlation to C-10 (δ_C

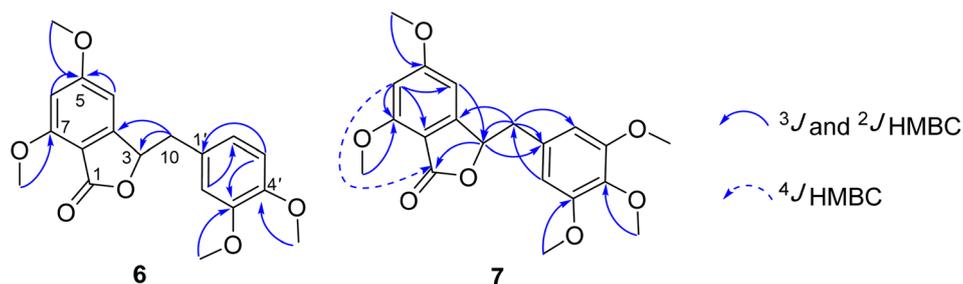**Fig. 2** Selected HMBC correlations of **6** and **7**.

Table 1 ^{1}H NMR (500 MHz, δ_H, multi, (J in Hz)) and ^{13}C NMR (125 MHz) spectral data of **6–7** and julacelide in acetone-d_6

No.	Julacelide δ_H (multi, J in Hz)	δ_C	**6** δ_H (multi, J in Hz)	δ_C	**7** δ_H (multi, J in Hz)	δ_C
1		166.5		167.1		167.5
2	5.69 (dd, 6.0, 5.5)	80.5	5.85 (t, 6.0)	80.3	5.62 (dd, 6.5, 5.0)	80.2
3	7.05 (dd, 8.0, 2.0)	115.1	6.61 (s)	99.5	6.59 (d, 1.5)	99.7
4	7.65 (dd, 8.5, 8.0)	136.7		166.8		167.4
5	7.05 (dd, 8.0, 2.0)	111.8	6.54 (d, 2.0)	99.6	6.54 (d, 1.5)	99.4
6		159.3		160.3		160.4
7		123.5		105.1		107.8
8		153.2		154.8		155.3
9	3.25 (dd, 14.5, 5.0), 3.12 (dd, 14.0, 6.0)	40.6	3.25 (dd, 14.0, 5.0), 3.10 (dd, 14.0, 6.0)	40.6	3.25 (dd, 14.5, 5.0), 3.10 (dd, 14.5, 6.5)	41.4
1′		129.1		129.3		132.6
2′	6.82 (d, 2.0)	114.6	6.87 (d, 1.5)	114.6	6.58 (s)	108.2
3′		150.0		150.0		154.1
4′		149.3		148.3		137.2
5′	6.80 (d, 8.0)	112.5	6.82 (d, 8.0)	112.6		154.1
6′	6.73 (dd, 8.0, 2.0)	122.9	6.77 (dd, 8.5, 2.0)	122.9	6.57 (s)	108.2
5-OCH$_3$			3.87 (s)	56.4	3.88 (s)	56.4
7-OCH$_3$	3.89 (s)	56.0	3.89 (s)	56.0	3.87 (s)	56.2
3′-OCH$_3$	3.74 (s)	56.0	3.75 (s)	56.3	3.75 (s)	56.4
4′-OCH$_3$	3.71 (s)	56.1	3.73 (s)	56.4	3.67 (s)	60.5
5′-OCH$_3$					3.75 (s)	56.4

47.9), while H-10 gave HMBC correlations to C-19 and C-20, supporting the position of H-20. Moreover, H$_3$-20 and H$_3$-17 (δ_H 0.78) gave HMBC correlations to the same carbons, C-8 (δ_C 37.4) and C-9 (δ_C 40.3), indicating their locations. A vinyl group was defined to attach at C-13 due to HMBC correlations of H$_3$-16 (δ_H 1.24), H$_2$-15 (δ_H 5.21 and 4.98), and H-14 (δ_H 5.93) to C-13 (δ_C 72.8) (Fig. 4). The NMR data of **8** were highly similar to those of (−)-roseostachenone[35] and 13-*epi*-(−)-roseostachenone,[36] indicating that they shared the same planar structure. The difference between them was easily observed in the change of the chemical shifts of H$_3$-19 (δ_H 1.25 in **8** *vs.* 1.06 in (−)-roseostachenone and 13-*epi*-(−)-roseostachenone) and CH$_3$-20 (δ_H 0.58 in **8** *vs.* 0.76 in (−)-roseostachenone and 13-*epi*-(−)-roseostachenone) recorded in the same deuterated solvent (CDCl$_3$). This finding proposes that **8** should have a *cis*-clerodane skeleton rather than a *trans*-clerodane of (−)-roseostachenone and 13-*epi*-(−)-roseostachenone. NOESY correlations (in CDCl$_3$) of H$_3$-17 (δ_H 0.77)/H$_3$-20 (δ_H 0.58)/H-1a (δ_H 2.50) indicated their same orientation. In contrast, NOESY correlations of H$_3$-19 (δ_H 1.25)/H-10 (δ_H 1.83)/H-1b (δ_H 2.69) indicated their same β-face. The downfield ^{13}C chemical shift of C-19 at δ_C 32.3 also supported the *cis* conjunction of H-10 and H$_3$-19.[33,34] Combined, the chemical structure of **8** was elucidated as shown in Fig. 1, namely marchanol.

2.1   Alpha-glucosidase inhibition and kinetic study

Compounds **1–5** and **10–12** displayed strong inhibition, with IC$_{50}$ values ranging from 28.9 to 130.6 μM, while compounds **6–9** showed weak activity (Table 3). Alpha-glucosidase inhibition of compounds **13–15** was previously evaluated in many published reports.[37] Among the tested compounds, bis-bibenzyl-type compounds **1–4** showed better inhibition. The main difference between **1–4** is in the linkage between C- and D-rings (Fig. 1). The ether connection in **1** and **4** might significantly decrease the activity, compared to the direct connection in **2–3**. The activity of **2** was stronger than **3**, indicating the important role of connectivity between C- and D-rings. The bis-bibenzyl series showed strong cytotoxicity against many cancer cell lines.[38] Nevertheless, fewer studies about the alpha-glucosidase inhibition of this series were conducted. Only marchantin C and riccardin C have been investigated so far.[38] In 2008, Dodo and co-workers reported the alpha-glucosidase inhibition of riccardin C and their oxygenated analogues.[39] All tested compounds showed potent activity, with IC$_{50}$ values ranging from 4.9 to 49 μM.[39] While ursolic acid (**12**) were thought to be a potent alpha-glucosidase inhibitor, the activities of 12-oleanene-3-one (**10**) and 3,11-dioxoursolic acid (**11**) have not been reported.

The most active compound **2** was selected for the enzyme inhibitory kinetic analysis. To examine the inhibition mechanism, activity at concentrations of 0, 3.61, 7.22, 14.44, and 28.88 μM of **2** was recorded. Lineweaver–Burk plots of **2** gave a group of lines with the same Michaelis constant (K_m), intersecting the y-axis in the second quadrant (Fig. 5A and B). Increasing inhibitor concentrations cause a decrease in the V_{max} of α-glucosidase. The kinetics of enzyme inhibition showed that **2** acted as a non-competitive inhibitor. The K_i value of **2** was determined as 67.1 ± 1.28 μM, respectively.

2.2   *In silico* docking study

The estimated binding energies of synthesized compounds to 4J5T protein obtained from 250 runs each per complex have

Table 2 ¹H and ¹³C NMR spectral data of **8**, (−)-roseostachenone and 13-*epi*-(−)-roseostachenone

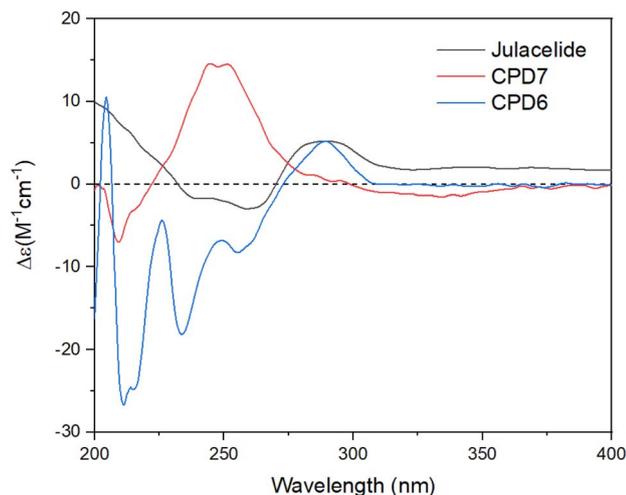| No.	8 δ_H (multi, J in Hz) (acetone-d_6, 500 MHz)	8 δ_H (multi, J in Hz) (CDCl$_3$, 500 MHz)	8 δ_C (acetone-d_6, 125 MHz)	(−)-Roseostachenone δ_H (multi, J in Hz) (CDCl$_3$, 200 MHz)	(−)-Roseostachenone δ_C (CDCl$_3$, 50 MHz)	13-*epi*-(−)-Roseostachenone δ_H (multi, J in Hz) (CDCl$_3$, 200 MHz)	13-*epi*-(−)-Roseostachenone δ_C (CDCl$_3$, 50 MHz)
1	2.66 (dd, 18.5, 7.0), 2.43 (d, 18.0)	2.69 (dd, 18.5, 6.5), 2.50 (d, 18.5)	35.7	2.28 (m)	34.8	2.28 (m)	34.3
2			198.8		200.4		200.5
3	5.56 (d, 1.0)	5.84 (brs)	129.1	5.67 (m)	125.4	5.66 (d, 1.2)	127.4
4			169.4		172.5		172.6
5			40.1		39.7		39.7
6			37.5		34.8		35.5
7			29.1		26.8		26.8
8			37.4		35.8		35.8
9			40.3		38.3		38.3
10	1.90 (m)	1.83 (d, 6.5)	47.9	1.87 (m)	45.5		45.5
11			31.3		31.1		31.1
12			35.8		35.5		34.7
13			72.8		73.0		73.0
14	5.93 (dd, 17.0, 10.5)	5.87 (dd, 10.5, 17.5)	147.1	5.83 (dd, 10.70, 17.33)	144.9	5.82 (dd, 17.4, 10.7)	144.8
15	5.21 (dd, 17.5, 2.0), 4.98 (dd, 11.0, 2.0)	5.09 (d, 11.0), 5.20 (d, 16.5)	111.5	5.03 (dd, 10.7, 1.0), 5.16 (dd, 17.3, 1.0)	112.0	5.14 (dd, 17.4, 1.3), 5.03 (dd, 10.7, 1.3)	111.9
16	1.24 (s)	1.22 (s)	28.5	1.23 (s)	27.6	1.22 (s)	27.7
17	0.78 (d, 7.0)	0.77 (d, 7.0)	16.3	0.77 (d, 6.5)	15.8	0.79 (d, 6.8)	15.6
18	1.96 (d, 1.0)	1.94 (d, 1.5)	20.5	1.84 (d, 1.0)	18.9	1.83 (d, 1.1)	18.9
19	1.25 (s)	1.25 (s)	32.3	1.06 (s)	18.3	1.06 (s)	18.2
20	0.56 (s)	0.58 (s)	19.6	0.76 (s)	18.0	0.76 (s)	17.9

Fig. 3 ECD spectra of compounds **6**–**7** and julacelide.

shown highly identical values due to the structural rigidity of those ligands. Meanwhile, the **1** conformational clusters have been computed in the range of -8.17 to -8.26 kcal mol^{-1} for 172 runs out of 250, the **1a**, **2**, and **3** clusters have been resulted 250 values in the range of 9.37 to -7.74, -9.78 to -9.84, and -9.26 to -9.31 kcal mol^{-1}, respectively. The interactions of those complexes were shown in Fig. 6, while the best binding energy from the docking simulation could be found in Table 4. Compound **1** was strongly positioned by five H-bond interactions with 4J5T at Asp 392, Trp 391, Gly 566, Trp 710, Tyr 709. These interactions were also observed in the **1a**–4J5T complex, where the addition of the bromo substituent on **1a**, although not further generating an H-bond, increased the hydrophobic interaction with the region of Phe 385. That may be the reason why the binding energy of **1a** with 4J5T was slightly increased compared to **1**.

The ether structure of **3** showed a slight difference in the order of the aromatic nuclei as well as the deletion of a hydroxy group, which reduced the number of hydrogen bonds but ensured hydrophobic interactions. Only one H-bond with Asp 568 and one pi–pi stacking with Tyr 709 were the major interactions of **3**. Regarding **2**, the aromatic scaffolds of this structure were arranged in accordance with the pi–pi stacking regions of Phe 385, Phe 389, or Tyr 709. Therefore, unlike **1** or **1a**, compound **2** performed four H-bonds with Arg 387, Glu 429,

Asp 568, and Asp 569. This framework seemed most suitable for 4J5T inhibition in this series of cyclic ethers.

3. Material and methods

3.1 General experimental procedures

The NMR spectra were recorded on a Bruker Avance III spectrometer (500 MHz for ^{1}H NMR and 125 MHz for ^{13}C NMR). The HRESIMS was recorded using an HRESIMS MicrOTOF-Q mass spectrometer on an LC-Agilent 1100 LC-MSD Trap spectrometer. Thin layer chromatography (TLC) was carried out on pre-coated silica gel 60 F$_{254}$ or silica gel 60 RP-18 F$_{254S}$ (Merck). Spots were visualized by spraying with a 10% H$_2$SO$_4$ solution, followed by heating. Gravity-column chromatography was performed on silica gel 60 (0.040–0.063 mm, Himedia).

3.2 Plant material

Marchantia polymorpha L. was collected in Lam Dong Province, Vietnam, from January to March 2023. The specimen was deposited at the herbarium in the laboratory of the Faculty of Chemistry, Ho Chi Minh City University of Education, Vietnam (UE-021). The scientific name was defined by Dr Tram Nguyen Khanh Trinh, Faculty of Biology, Ho Chi Minh City University of Science.

3.3 Extraction and isolation of compounds

Dried, ground powder of *M. polymorpha* (4.5 kg) was extracted with EtOAc (3 × 10 L, each 8 hours) at room temperature. The obtained solution was filtered and evaporated to obtain a crude EtOAc extract (169.3 g). This extract was successively applied to a silica gel column chromatography (CC), isocratically eluted with *n*-hexane : EtOAc (1 : 1, v/v), to obtain six fractions, **EA1**–**EA6**. These fractions were evaluated for their alpha-glucosidase inhibition to choose the fractions for further analysis. The isolation of **1**–**15** were described in Scheme 1 using silica gel CC with various solvent systems.

3.3.1. Marchantin A (1). Yellow powder. C$_{28}$H$_{24}$O$_5$. ^{1}H NMR (500 MHz, CDCl$_3$, δ, ppm, *J*/Hz): 7.13 (1H, dd, *J* = 8.0, 7.5 Hz, H-11), 7.00 (1H, dd, *J* = 8.0, 1.5 Hz, H-10), 6.97 (1H, t, *J* = 7.8, H-13′), 6.91 (1H, d, *J* = 8.5 Hz, H-3), 6.91 (1H, d, *J* = 8.5 Hz, H-5), 6.85 (1H, dd, *J* = 8.0, 1.5 Hz, H-12), 6.57 (1H, d, *J* = 8.0 Hz, H-2), 6.57 (1H, d, *J* = 8.0 Hz, H-6), 6.57 (1H, dd, *J* = 2.5, 2.0 Hz, H-10′), 6.53 (1H, dd, *J* = 8.5, 2.0 Hz, H-12′), 6.46 (1H, d, *J* = 1.5 Hz, H-5′), 6.39 (1H, brd, *J* = 7.5 Hz, H-14′), 5.13 (1H, d, *J* = 1.5 Hz, H-3′),
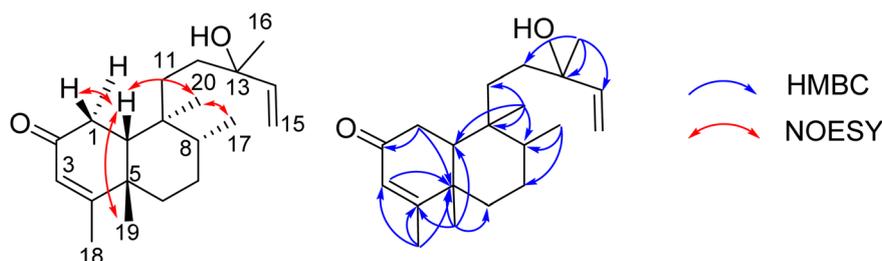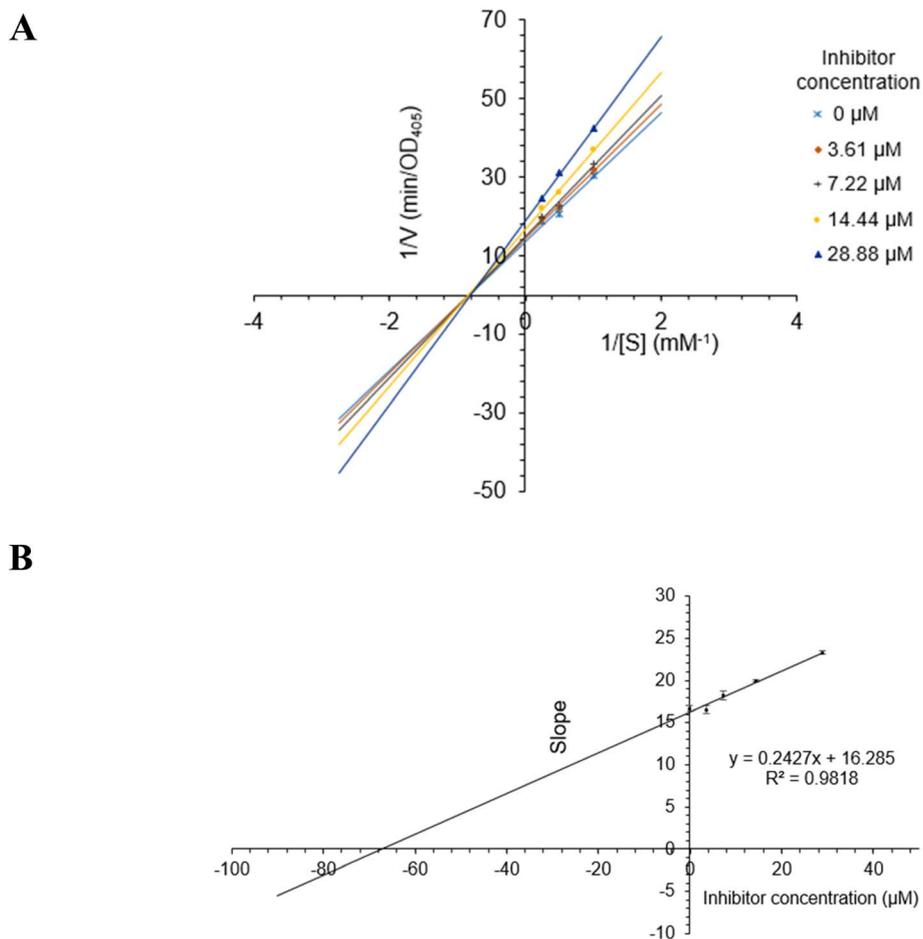

Fig. 4 Selected HMBC and NOESY correlations of **8**.

Paper

Fig. 5 (A) Lineweaver–Burk plot for alpha-glucosidase inhibition by **2**. (B) Plots of slope *versus* concentration of **2** for the determination of the inhibition constant K_i.

2.97–3.01 (2H, m, H-7, H-8), 2.78–2.80 (2H, m, H-7′), 2.72–2.74 (2H, m, H-8′). ^{13}C NMR (125 MHz, CDCl$_3$, δ, ppm): 156.8 (C-11′), 153.2 (C-1), 148.7 (C-13), 146.5 (C-2′), 144.3 (C-6′), 143.1 (C-9′), 139.7 (C-14), 139.1 (C-4), 136.2 (C-9), 132.5 (C-4′), 130.8 (C-1′), 129.6 (C-3), 129.6 (C-5), 128.9 (C-13′), 126.0 (C-11), 123.2 (C-14′),

121.9 (C-10), 121.2 (C-2), 121.2 (C-6), 115.5 (C-10′), 114.4 (C-12), 112.0 (C-12′), 109.3 (C-5′), 107.9 (C-3′), 35.5 (C-8′), 35.3 (C-7), 34.1 (C-7′), 30.3 (C-8).

3.3.2. Isoriccardin C (2). Yellow powder. C$_{28}$H$_{26}$O$_4$. ^{1}H NMR (500 MHz, acetone-d_6, δ, ppm, J/Hz): 7.13 (1H, dd, J = 7.5, 2.5 Hz, H-5), 7.10 (1H, dd, J = 7.5, 2.5 Hz, H-3), 7.305 (1H, t, J = 8.0 Hz, H-13′), 6.86 (1H, d, J = 7.5 Hz, H-12′), 6.82 (1H, d, J = 8.5 Hz, H-2), 6.81 (1H, d, J = 8.5 Hz, H-6), 6.81 (1H, m, H-13), 6.74 (1H, d, J = 8.0 Hz, H-6′), 6.70 (1H, dd, J = 8.0, 2.0 Hz, H-14′), 6.69 (1H, dd, J = 8.0, 2.0 Hz, H-5′), 6.65 (1H, brs, H-10), 6.54 (1H, d, J = 7.5 Hz, H-14), 5.73 (1H, d, J = 1.0 Hz, H-3′), 3.02–3.16 (4H, m, H-7, H-8), 2.50–2.64 (2H, m, H-8′), 2.30–2.33 (2H, m, H-7′). ^{13}C NMR (125 MHz, acetone-d_6, δ, ppm): 206.1 (C-11′), 177.1 (C-12), 155.5 (C-1), 154.9 (C-11), 145.5 (C-2′), 143.4 (C-1′), 142.1 (C-9), 138.1 (C-4), 138.1 (C-9′), 134.6 (C-4′), 131.9 (C-3), 131.6 (C-13), 131.4 (C-5), 129.1 (C-13′), 122.4 (C-14), 122.1 (C-2), 122.1 (C-6), 121.6 (C-5′), 121.6 (C-14′), 120.5 (C-10′), 117.5 (C-10), 116.4 (C-3′), 116.3 (C-6′), 113.7 (C-12′), 38.5 (C-7′), 37.6 (C-8′), 36.8 (C-8), 35.4 (C-7).

3.3.3. Riccardin C (3). Yellow powder. C$_{28}$H$_{26}$O$_4$. ^{1}H NMR (500 MHz, acetone-d_6, δ, ppm, J/Hz): 7.03 (1H, t, J = 8.0 Hz, H-13), 6.95 (1H, t, J = 8.0 Hz, H-3), 6.95 (1H, t, J = 8.0 Hz, H-5),

Table 3 Alpha-glucosidase inhibition (IC$_{50}$) of the test compounds

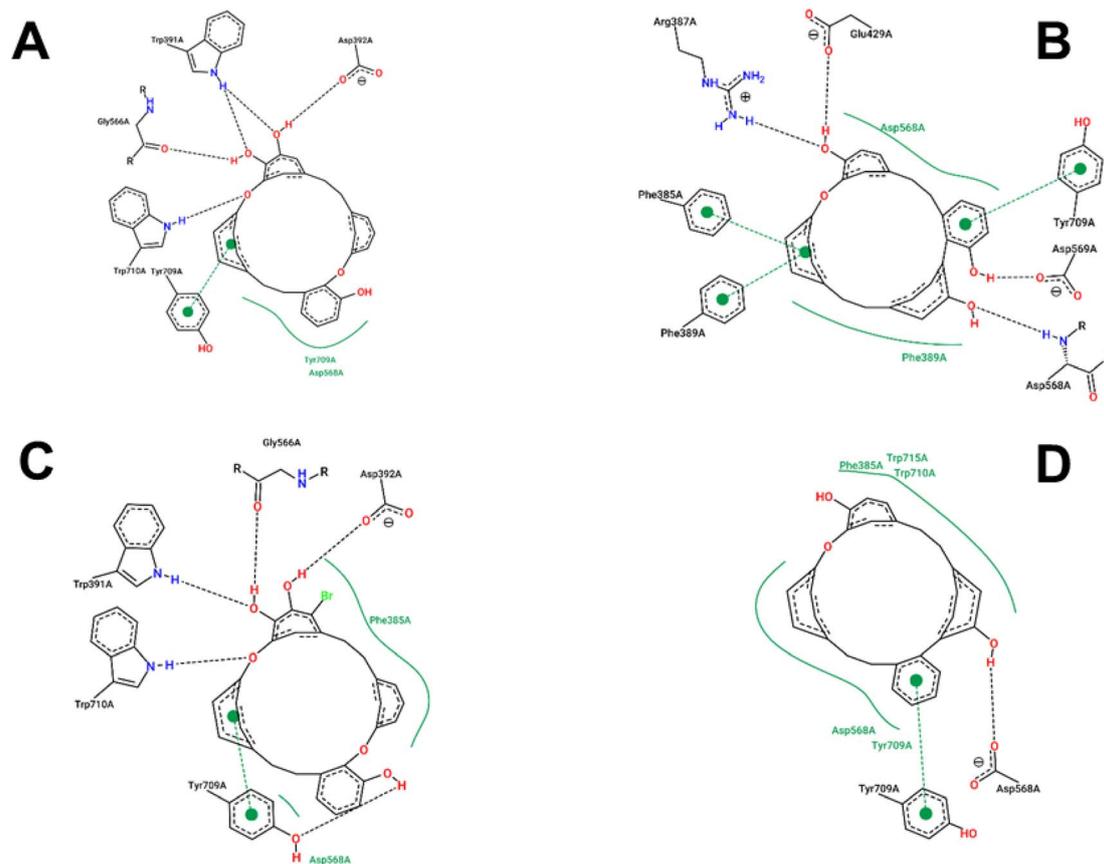| Bio-source		IC$_{50}$ (μM)
Compound	**1**	57.3 ± 1.9
	1a	150.6 ± 2.9
	2	28.9 ± 0.2
	3	42.2 ± 1.4
	4	130.6 ± 3.0
	5	129.5 ± 2.0
	6	>200
	7	>200
	8	>200
	9	>200
	10	75.1 ± 1.8
	11	101.0 ± 3.0
	12	86.0 ± 6.9
Positive control	Acarbose	330.9 ± 4.2

Fig. 6 **1**−4J5T (A), **2**−4J5T (B), **1a**−4J5T (C) and **3**−4J5T (D) interactions.

6.93 (1H, m, H-10), 6.77 (1H, d, $J = 8.0$ Hz, H-11′), 6.73 (1H, m, H-2), 6.73 (1H, m, H-6), 6.73 (1H, m, H-12), 6.72 (1H, d, $J = 8.0$ Hz, H-6′), 6.50 (1H, m, H-5′), 5.36 (1H, d, H-3′), 2.63–3.03 (m, H-7, H-8, H-7′, H-8′). ^{13}C NMR (100 MHz, acetone-d_6, δ, ppm): 157.8 (C-11), 154.4 (C-1), 154.1 (C-13′), 148.0 (C-2′), 145.4 (C-1′), 144.3 (C-9), 141.8 (C-9′), 140.8 (C-4), 133.5 (C-4′), 133.4 (C-13), 133.1 (C-11′), 130.3 (C-3), 130.3 (C-5), 128.9 (C-14), 126.8 (C-12′), 122.9 (C-2), 122.9 (C-6), 122.7 (C-10′), 121.5 (C-5′), 117.7 (C-10), 117.4 (C-14′), 116.6 (C-6′), 114.0 (C-12), 38.7 (C-7), 38.5 (C-8′), 37.9 (C-7′), 36.0 (C-8).

3.3.4. Marchantin K (4). White amorphous powder. $C_{29}H_{28}O_7$. ^{1}H NMR (500 MHz, acetone-d_6, δ, ppm, J/Hz): 6.95 (1H, brd, $J = 8.0$ Hz, H-3), 6.95 (1H, brd, $J = 8.0$ Hz, H-5), 6.88 (1H, t, $J = 7.5$ Hz, H-13′), 6.82 (1H, dd, $J = 8.0$, 1.5 Hz, H-10), 6.93 (1H, m, H-10), 6.76 (1H, d, $J = 8.5$ Hz, H-11), 6.68 (1H, d, $J =$

2.0 Hz, H-10′), 6.59 (1H, d, $J = 2.0$ Hz, H-5′), 6.51 (1H, brd, $J = 8.0$ Hz, H-2), 6.51 (1H, brd, $J = 8.0$ Hz, H-6), 6.45 (1H, dd, $J = 8.5$, 3.0 Hz, H-12′), 6.05 (1H, brd, $J = 7.0$ Hz, H-14′), 4.97 (1H, d, $J = 2.0$ Hz, H-3′), 4.08 (1H, dd, $J = 9.5$, 4.0 Hz, H-7′), 3.20 (s, –OMe), 3.09–3.14 (1H, m, H-7a), 2.95–3.06 (1H, m, H-7b), 2.95–3.06 (2H, m, H-8) 3.00 (1H, m, H-8′a), 2.59 (1H, dd, $J = 13.0$, 10.0 Hz, H-8′b). ^{13}C NMR (125 MHz, acetone-d_6, δ, ppm): 157.6 (C-11′), 153.9 (C-1), 149.9 (C-2′), 147.3 (C-6′), 147.1 (C-12), 146.3 (C-14), 140.0 (C-4), 139.1 (C-9′), 138.8 (C-13), 136.8 (C-1′) 133.3 (C-4′), 131.4 (C-9), 129.4 (C-3), 129.4 (C-5), 127.8 (C-13′), 125.5 (C-14′), 123.4 (C-2), 121.4 (C-6), 120.9 (C-10), 116.9 (C-10′), 114.4 (C-12′), 112.3 (C-11), 107.6 (C-3′), 106.0 (C-5′), 84.1 (C-7′), 43.8 (C-8′), 35.5 (C-7), 30.1 (C-8).

3.3.5. Lunularin (5). White amorphous solid. $C_{14}H_{14}O_2$. ^{1}H NMR (500 MHz, acetone-d_6, δ, ppm, J/Hz): 7.07 (1H, t, $J = 7.8$ Hz, H-5′), 7.03 (1H, d, $J = 8.0$ Hz, H-3), 7.03 (1H, d, $J = 8.0$ Hz, H-5), 6.73 (1H, d, $J = 8.5$ Hz, H-2), 6.73 (1H, d, $J = 8.5$ Hz, H-6), 6.69 (1H, d, $J = 2.0$ Hz, H-4′), 6.67 (1H, s, H-2′), 6.63 (1H, d, $J = 8.0$ Hz, H-6′), 2.78 (2H, s, H-7), 2.78 (2H, s, H-8). ^{13}C NMR (125 MHz, acetone-d_6, δ, ppm): 157.4 (C-3′), 155.5 (C-1), 143.6 (C-1′), 132.6 (C-4), 129.3 (C-5′), 129.1 (C-3), 129.1 (C-5), 119.5 (C-6′), 115.4 (C-3′), 115.0 (C-2), 115.0 (C-6), 112.7 (C-4′), 38.1 (C-8), 36.8 (C-7).

3.3.6. 3R-(3,4-Dimethoxybenzyl)-5,7-dimethoxyphthalide (6). Colorless oil. $C_{19}H_{20}O_6$. ^{1}H NMR (500 MHz, acetone-d_6, δ, ppm, J/Hz): 6.87 (1H, d, $J = 1.5$ Hz, H-2′), 6.82 (1H, d, $J = 8.0$ Hz, H-5′), 6.77 (1H, dd, $J = 8.5$, 2.0 Hz, H-6′), 6.61 (1H, s, H-4),

Table 4 The best binding energy between ligands and the 4J5T protein

Ligand	Best binding energy from docking (kcal mol^{-1})
1	−8.26
1a	−9.74
2	−9.84
3	−9.31

6.54 (1H, d, J = 2.0 Hz, H-6), 5.85 (1H, t, J = 6.0 Hz, H-3), 3.89 (3H, s, 7-OCH$_3$), 3.87 (3H, s, 5-OCH$_3$), 3.75 (3H, s, 3′-OCH$_3$), 3.73 (3H, s, 4′-OCH$_3$), 3.25 (1H, dd, J = 14.0, 5.0 Hz, H-10a), 3.10 (1H, dd, J = 14.0, 5.0 Hz, H-10b). ^{13}C NMR (125 MHz, acetone-d_6, δ, ppm): 167.1 (C-1), 167.1 (C-5), 160.3 (C-7), 154.8 (C-9), 150.0 (C-3′), 148.3 (C-4′), 129.3 (C-1′), 122.9 (C-6′), 114.6 (C-2′), 112.6 (C-5′), 105.1 (C-8), 99.6 (C-6), 99.5 (C-4), 99.5 (C-3), 56.4 (5-OCH$_3$), 56.4 (4′-OCH$_3$), 56.3 (3′-OCH$_3$), 56.0 (7-OCH$_3$).

3.3.7. Marchatoside (7). Colorless oil. C$_{20}$H$_{22}$O$_7$. HRESIMS m/z: 375.1397 [M + H]$^+$ (calcd for C$_{20}$H$_{23}$O$_7^+$, 375.1443). ^{1}H NMR (500 MHz, acetone-d_6, δ, ppm, J/Hz) and ^{13}C NMR (125 MHz, acetone-d_6, δ, ppm) data: see Table 1.

3.3.8. Marchanol (8). Colorless oil. C$_{20}$H$_{32}$O$_2$. HRESIMS m/z: 327.2295 [M + Na]$^+$ (calcd for C$_{20}$H$_{32}$O$_2$Na$^+$, 327.2300). ^{1}H NMR (500 MHz, acetone-d_6, δ, ppm, J/Hz) and ^{13}C NMR (125 MHz, acetone-d_6, δ, ppm) data: see Table 2.

3.3.9. Vitexilactone (9). Colorless oil. C$_{22}$H$_{34}$O$_4$. ^{1}H NMR (500 MHz, acetone-d_6, δ, ppm, J/Hz): 5.86 (1H, p, J = 1.5, 1.5, 2.0, 2.0 Hz, H-14), 5.34 (1H, q, J = 3.0, 3.0, 2.5 Hz, H-6), 4.85 (1H, d, J = 2.0 Hz, H-16), 2.61 (2H, m, H-12), 2.17 (1H, m, H-8), 2.02 (1H, m, H-9), 2.00 (1H, s, H-2′), 1.85 (1H, q, J = 6.5, 4.5 3.0 Hz, H-11a), 1.82 (1H, q, J = 4.0, 4.0, 6.5 Hz, H-11b), 1.76 (1H, d, 2.5 Hz, H-5), 1.71–1.50 (2H, m, H-2), 1.47–1.44 (2H, m, H-7), 1.43–1.32 (2H, m, H-1), 1.37–1.24 (2H, m, H-3), 1.30 (3H, s, 20-CH$_3$), 1.02 (3H, s, 19-CH$_3$), 0.93 (3H, s, 18-CH$_3$), 0.92 (3H, s, 17-CH$_3$). ^{13}C NMR (125 MHz, acetone-d_6, δ, ppm): 174.0 (C-15), 173.4 (C-13), 170.5

(C-1′), 114.8 (C-14), 73.8 (C-16), 70.4 (C-6), 44.7 (C-10), 45.6 (C-5), 43.0 (C-3), 37.4 (C-7), 36.9 (C-9), 34.7 (C-4), 34.0 (C-18), 32.8 (C-8), 32.6 (C-11), 32.5 (C-1), 26.0 (C-12), 24.1 (C-19), 21.8 (C-2′), 19.6 (C-2), 19.5 (C-20), 16.4 (C-17).

3.3.10. 12-Oleanene-3-one (10). Yellow amorphous powder. C$_{20}$H$_{20}$O$_8$. ^{1}H NMR (500 MHz, acetone-d_6, δ, ppm, J/Hz): 5.24 (1H, t, J = 4.0 Hz, H-12), 2.31 (1H, m, H-9), 1.19 (3H, s, H-27), 1.10 (3H, s, H-25), 1.06 (3H, s, H-26), 1.05 (3H, s, H-24), 1.03 (3H, s, H-23), 0.89 (3H, s, H-29), 0.86 (3H, s, H-30), 0.84 (3H, s, H-28). ^{1}H NMR (500 MHz, CDCl$_3$, δ, ppm, J/Hz): 5.21 (1H, t, J = 3.5, 4.0 Hz, H-12), 2.37 (1H, m, H-9), 1.25 (3H, s, H-27), 1.07 (3H, s, H-24), 1.06 (3H, s, H-23), 1.02 (3H, s, H-25), 1.00 (3H, s, H-26), 0.92 (3H, s, H-29), 0.87 (3H, s, H-30), 0.84 (3H, s, H-28). ^{13}C NMR (125 MHz, acetone-d_6, δ, ppm): 216.2 (C-3), 146.0 (C-13), 122.8 (C-12), 56.0 (C-5), 47.8 (C-9), 47.7 (C-4), 47.3 (C-19), 47.0 (C-18), 41.9 (C-14), 40.0 (C-7), 39.8 (C-1), 37.1 (C-22), 35.5 (C-10), 34.7 (C-2), 34.7 (C-21), 33.1 (C-7), 32.3 (C-17), 32.3 (C-30), 31.3 (C-20), 28.9 (C-28), 26.9 (C-16), 26.4 (C-15), 26.4 (C-23), 24.6 (C-27), 23.7 (C-29), 23.7 (C-11), 21.9 (C-24), 20.4 (C-6), 17.3 (C-26), 15.6 (C-25).

3.3.11. 3,11-Dioxoursolic acid (11). White amorphous powder. C$_{30}$H$_{44}$O$_4$. ^{1}H NMR (400 MHz, CDCl$_3$, δ, ppm, J/Hz): 5.63 (1H, s, H-12), 2.39 (1H, s, H-9), 1.31 (3H, s, H-27), 1.24 (3H, s, H-26), 1.02 (3H, s, H-25), 0.97 (3H, d, J = 8.0 Hz, H-30), 0.95 (3H, s, H-24), 0.90 (3H, s, H-23), 0.87 (3H, d, J = 8.0 Hz, H-29). ^{13}C NMR (100 MHz, acetone-d_6, δ, ppm): 217.4 (C-3),
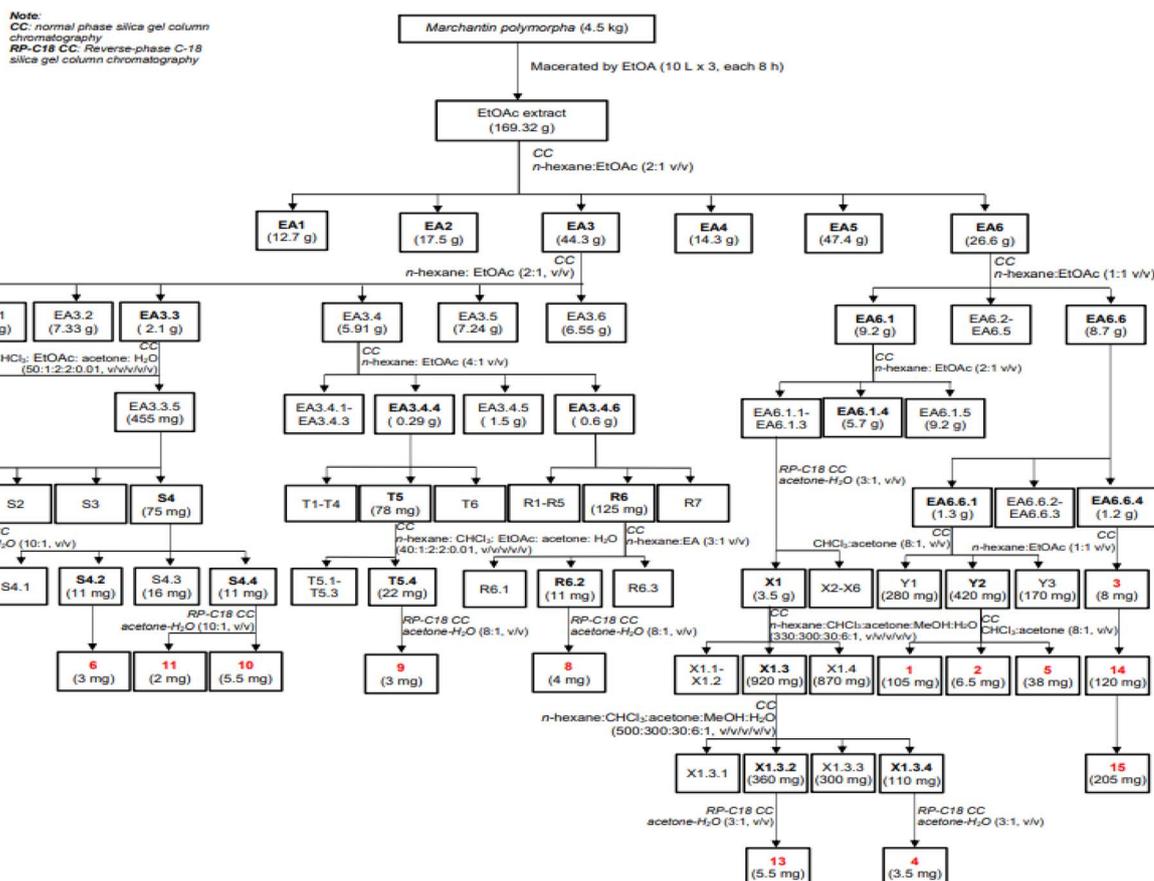
Scheme 1 Isolation procedure of compounds **1–15**.

199.5 (C-11), 182.8 (C-28), 163.3 (C-13), 130.8 (C-12), 60.8 (C-9), 55.5 (C-5), 52.6 (C-8), 47.9 (C-4), 47.6 (C-17), 44.0 (C-14), 41.5 (C-19), 41.5 (C-20), 39.9 (C-8), 38.7 (C-1), 36.9 (C-10), 36.1 (C-22), 34.3 (C-2), 32.5 (C-7), 28.6 (C-15), 26.6 (C-21), 26.6 (C-23), 23.8 (C-16), 23.7 (C-29), 21.2 (C-24), 21.1 (C-27), 19.0 (C-6), 18.8 (C-26), 17.2 (C-30), 15.7 (C-25).

3.3.12. Ursolic acid (12). White amorphous powder. $C_{30}H_{48}O_3$. ^{1}H NMR (500 MHz, CDCl$_3$, δ, ppm, J/Hz): 5.26 (1H, t, J = 3.5 Hz, H-12), 3.22 (1H, dd, J = 7.0, 5.0, 4.0 Hz, H-3), 2.19 (1H, d, J = 11.5, H-18), 1.02 (3H, s, H-27), 0.92 (3H, s, H-23), 0.86 (3H, d, J = 6.5 Hz, H-29), 0.85 (3H, s, H-26), 0.80 (3H, s, H-25), 0.77 (3H, d, J = 4.0 Hz, H-30), 0.77 (3H, s, H-24). ^{13}C NMR (125 MHz, CDCl$_3$, δ, ppm): 182.8 (C-28), 138.1 (C-13), 126.0 (C-12), 79.2 (C-3), 55.4 (C-5), 53.0 (C-18), 48.0 (C-17), 47.7 (C-9), 42.2 (C-14), 41.7 (C-19), 39.6 (C-8), 39.6 (C-20), 39.0 (C-4), 38.9 (C-1), 36.8 (C-10), 36.8 (C-22), 33.2 (C-7), 30.8 (C-21), 30.8 (C-15), 28.3 (C-23), 27.4 (C-2), 24.4 (C-16), 23.7 (C-11), 23.7 (C-27), 21.3 (C-30), 18.5 (C-6), 17.2 (C-26), 17.1 (C-29), 15.8 (C-25), 15.6 (C-24).

3.3.13. Artemetin (13). Yellow amorphous powder. $C_{20}H_{20}O_8$. ^{1}H NMR (500 MHz, acetone-d_6, δ, ppm, J/Hz): 12.69 (1H, s, 5-OH), 7.78 (1H, d, J = 2.0 Hz, H-2′), 7.76 (1H, dd, J = 3.0, 2.0 Hz, H-6′), 7.14 (1H, d, J = 8.5 Hz, H-5′), 6.81 (1H, s, H-8), 3.96 (3H, s, 6-OCH$_3$), 3.92 (3H, s, 3-OCH$_3$), 3.90 (6H, s, 7-OCH$_3$, 3′-OCH$_3$), 3.80 (3H, s, 4′-OCH$_3$). ^{13}C NMR (125 MHz, acetone-d_6, δ, ppm): 178.9 (C-4), 159.3 (C-7), 155.8 (C-2), 152.7 (C-5), 152.3 (C-8a), 152.0 (C-4′), 149.2 (C-3′), 138.6 (C-3), 132.3 (C-6), 122.8 (C-1′), 122.1 (C-2′), 111.8 (C-6′), 111.3 (C-5′), 106.2 (C-4a), 90.8 (C-8), 59.7 (7-OCH$_3$), 59.4 (3-OCH$_3$), 55.9 (6-OCH$_3$), 55.4 (3′-OCH$_3$), 55.3 (4′-OCH$_3$).

3.3.14. 5′-Bromomarchantin A (1a). Colorless oil. $C_{28}H_{23}BrO_5$. HRESIMS m/z: 601.0543 [M − H]$^-$ (calcd for $C_{28}H_{22}BrO_5{}^-$, 517, 06506). ^{1}H NMR (500 MHz, acetone-d_6, δ, ppm, J/Hz): 7.10 (1H, t, J = 7.8 Hz, H-13′), 7.04 (1H, dd, J = 8.0, 1.5 Hz, H-12′), 7.00 (1H, t, J = 8.0 Hz, H-11), 6.96 (1H, d, J = 8.0 Hz, H-5), 6.96 (1H, d, J = 8.0 Hz, H-3), 6.82 (1H, dd, J = 8.0, 1.5 Hz, H-10), 6.61 (1H, dd, J = 8.5, 2.5 Hz, H-12), 6.50 (1H, d, J = 7.5 Hz, H-2), 6.50 (1H, d, J = 7.5 Hz, H-6), 6.28 (1H, d, J = 7.5 Hz, H-10′), 6.28 (1H, d, J = 7.5 Hz, H-14′), 5.34 (1H, s, H-3′), 3.02–3.06 (4H, m, H-7), 3.02–3.06 (4H, m, H-8), 2.91–2.93 (2H, m, H-7′), 2.91–2.93 (2H, m, H-8′). ^{13}C NMR (125 MHz, CDCl$_3$, δ, ppm): 158.7 (C-11′), 154.1 (C-1), 147.0 (C-2′), 144.5 (C-6′), 142.4 (C-14), 142.4 (C-9′), 139.5 (C-1′), 137.1 (C-4), 133.8 (C-4′), 130.7 (C-9), 130.5 (C-13′), 129.1 (C-3), 129.1 (C-5), 126.4 (C-14′), 122.1 (C-11), 121.8 (C-2), 121.8 (C-6), 121.5 (C-10), 118.5 (C-13), 116.5 (C-12′), 115.2 (C-10′), 113.8 (C-12), 109.6 (C-3′), 105.0 (C-5′), 35.7 (C-7), 35.7 (C-8′), 34.8 (C-7′), 34.1 (C-8).

3.4 Alpha-glucosidase inhibition assay

Evaluation of the inhibitory activity of **1**–**12** against yeast alpha-glucosidase followed a previous procedure.[37]

3.5 Kinetic study of α-glucosidase inhibition of 2

The mechanisms of inhibition of alpha-glucosidase by **2** were determined by Lineweaver–Burk plots (Microsoft Excel 2010, Washington, USA), using methods similar to those reported in the literature.[40] Enzyme inhibition due to various concentrations of **2** was evaluated by monitoring the effects of different concentrations of the substrate. For Lineweaver–Burk double reciprocal plots 1/enzyme velocity (1/V) vs. 1/substrate concentration (1/[S]), the inhibition type was determined using various concentrations of pNPG (1 mM, 2 mM, and 4 mM) as a substrate in the presence of different concentrations of the test compound (0, 3.61, 7.22, 14.44, and 28.88 μM for **2**). The experiments were carried out in three replicates. The mixtures were incubated at 37 °C, and the optical density was measured at 405 nm every 1 min for 30 min with the ELx800 Absorbance Microplate Reader (BioTek Instruments, Inc., Vermont, USA). The optimal concentrations of the tested compound were chosen based on the IC$_{50}$ value. The inhibition constants were obtained graphically from secondary plots (Microsoft Excel 2010, Washington, USA).

3.6 In silico molecular docking model

The 4J5T PDB structure from the Protein Data Bank was used to represent alpha-glucosidase in the docking study. The proteins and ligands were processed to calculate hydrogen bonds and Gasteiger–Marsili charges,[41] then converted into PDBQT format using AutodockTools. Herein, AutoDock 4.2 was employed for the simulations of protein–ligand complexes. The docking study was modeled with 250 genetic algorithm runs with 25 000 000 maximum number of evals (long mode). The lowest binding energies among the conformational clusters were extracted as the best-estimated docking value. The interactions of the docked conformations were analyzed via the Poseview tool.[42]

4. Conclusions

Two new compounds, marchatoside (**7**) and marchanol (**8**), were isolated from the liverwort *Marchantia polymorpha*. Additionally, thirteen known compounds, including marchantin A (**1**), isoriccardin C (**2**), riccardin C (**3**), marchantin K (**4**), lunularin (**5**), 3R-(3,4-dimethoxybenzyl)-5,7-dimethoxyphthalide (**6**), vitexilactone (**9**), 12-oleanene-3-one (**10**), 3,11-dioxoursolic acid (**11**), ursolic acid (**12**), artemetin (**13**), kaempferol (**14**), and quercetin (**15**), were also isolated and their structures were determined using a bio-guided procedure. Compounds **1**–**12** were evaluated for their alpha-glucosidase inhibition. The most active compound, compound **2**, was subsequently chosen for a kinetic study. It was determined to be of the non-competitive type. The inhibitory mechanism of compounds **1**–**4** was confirmed through a molecular docking study.

Conflicts of interest

No potential conflict of interest was reported by the authors.

Acknowledgements

References

1 D. Gahtori and P. Chaturvedi, Antifungal and antibacterial potential of methanol and chloroform extracts of *Marchantia polymorpha* L., *Arch. Phytopathol. Plant Prot.*, 2011, **44**, 726–731, DOI: **10.1080/03235408.2010.516083**.

2 S. Chandra, D. Chandra, A. Barh, B. Pankaj, R. K. Pandey and I. P. Sharma, Bryophytes: hoard of remedies, an ethno-medicinal review, *J. Tradit. Complementary Med.*, 2017, **7**, 94–98, DOI: **10.1016/j.jtcme.2016.01.007**.

3 Y. Asakawa, M. Tori, T. Masuya and J.-P. Frahm, Ent-sesquiterpenoids and cyclic bis(bibenzyls) from the german liverwort *Marchantia Polymorpha*, *Phytochemistry*, 1990, **29**, 1577–1584, DOI: **10.1016/0031-9422(90)80125-Z**.

4 M. Tori, K. Takikawa, H. G. Krishnamurty and S. K. Kar, Cyclic bis(bibenzyls) and related compounds from the liverworts *Marchantia polymorpha* and *Marchantia palmata*, *Phytochemistry*, 1987, **26**, 1811–1816, DOI: **10.1016/S0031-9422(00)82294-3**.

5 K. R. Markham and I. J. Porter, Flavonoids of the liverwort *Marchantia polymorpha*, *Phytochemistry*, 1974, **13**(9), 1937–1942, DOI: **10.1016/0031-9422(74)85120-4**.

6 A. Matsuo, N. Nakayama and M. Nakayama, Enantiomeric type sesquiterpenoids of the liverwort *Marchantia polymorpha*, *Phytochemistry*, 1985, **24**, 777–781, DOI: **10.1016/S0031-9422(00)84893-1**.

7 J.-B. Qu, C.-F. Xie, M. Ji, Y.-Q. Shi and H.-X. Lou, Water-soluble constituents from the liverwort *Marchantia polymorpha*, *Helv. Chim. Acta*, 2007, **90**, 2109–2115, DOI: **10.1002/hlca.200790218**.

8 S. Jensen, S. Omarsdottir, A. G. Bwalya, M. A. Nielsen, D. Tasdemir and E. S. Olafsdottir, Marchantin A, a macrocyclic bisbibenzyl ether, isolated from the liverwort *Marchantia polymorpha*, inhibits protozoal growth in vitro, *Phytomedicine*, 2012, **19**(13), 1191–1195.

9 N. Mewari and P. Kumar, Antimicrobial activity of extracts of *Marchantia polymorpha*, *Pharm. Biol.*, 2008, **46**, 819–822, DOI: **10.1080/13880200802315725**.

10 L. Fang, H.-F. Guo and H.-X. Lou, Three new bibenzyl derivatives from the Chinese liverwort *Marchantia polymorpha* L., *Helv. Chim. Acta*, 2007, **90**, 748–752, DOI: **10.1002/hlca.200790075**.

11 N. C. T. Son, T. Q. Tan, D. T. M. Lien, N. T. M. Huong, P. N. K. Tuyen, N. K. P. Phung, Q. N. D. Phuong and N. T. H. Thu, Five phenolic compounds from *Marchantia polymorpha* L. and their in vitro antibacterial, antioxidant and cytotoxic activities, *Vietnam J. Chem.*, 2020, **58**, 810–814, DOI: **10.1002/vjch.202000088**.

12 N. T. H. Le, N. C. T. Son, T. Q. Tan, N. K. P. Phung, Q. N. D. Phuong and N. T. H. Thu, Chemical investigation of the n-hexane extract of *Marchantia polymorpha* L, *VNUHCM Journal of Science and Technology Development*, 2022, **25**, 2308–2313, DOI: **10.32508/stdj.v25i1.3875**.

13 K. P. Adam and H. Becker, Phenanthrenes and other phenolics from in vitro cultures of *Marchantia polymorpha*, *Phytochemistry*, 1993, **35**, 139–143, DOI: **10.1016/S0031-9422(00)90522-3**.

14 A. Gökbulut, B. Satilmiş, K. Batçioğlu, B. Çetin and E. Şarer, Antioxidant activity and luteolin content of *Marchantia polymorpha* L, *Turk. J. Biol.*, 2012, **36**, 381–385, DOI: **10.3906/biy-1106-15**.

15 Y. Asakawa, M. Tori, K. Takikawa, H. G. Krishnamurty' and S. Kanti Kar, Cyclic bis(bibenzyls) and related compounds from the liverworts *Marchantia polymorpha* and *Marchantia palmata*, *Phytochemistry*, 1987, **26**, 1811–1816, DOI: **10.1016/S0031-9422(00)82294-3**.

16 T. Q. Tran, H. N. Phan, A. L. Bui and P. N. D. Quach, Biological activities of in vitro liverwort Marchantia polymorpha L. extracts, *Not. Bot. Horti Agrobot. Cluj-Napoca*, 2020, **48**, 826–838, DOI: **10.15835/NBHA48211884**.

17 T. Q. Tran, H. N. Phan, A. L. Bui and P. N. D. Quach, Khảo sát một số hoạt tính sinh học của loài địa tiền *Marchantia polymorpha* L. thu hái tại Đà Lạt, Lâm Đồng, *J. Nat. Sci.*, 2018, **2**, 26–34, DOI: **10.32508/stdjns.v2i5.774**.

18 Y. Asakawa, M. Toyota, M. Tori and T. Hashimoto, Chemical structures of macrocyclic bis(bibenzyls) isolated from liverworts (Hepaticae), *Spectroscopy*, 2000, **14**, 149–175, DOI: **10.1155/2000/570265**.

19 A. Bardón, N. Kamiya, M. Toyota, S. Takaoka and Y. Asakawa, Sesquiterpenoids, hopanoids and bis(bibenzyls) from the Argentine liverwort Plagiochasma rupestre, *Phytochemistry*, 1999, **52**, 1323–1329, DOI: **10.1016/S0031-9422(99)00452-5**.

20 L. Kraut, R. Mues and M. Sim-Sim, Sesquiterpene lactones and 3-benzylphthalides from Frullania muscicola, *Phytochemistry*, 1994, **37**, 1337–1346, DOI: **10.1016/S0031-9422(00)90409-6**.

21 M. Ono, M. Yamamoto, T. Yanaka, Y. Ito and T. Nohara, Ten new labdane-type diterpenes from the fruit of Vitex rotundifolia, *Chem. Pharm. Bull.*, 2001, **49**, 82–86, DOI: **10.1248/cpb.49.82**.

22 A. A. Matloub, M. A. Hamed and S. S. El Souda, Chemo-protective effect on hepato-renal toxicity and cytotoxic activity of lipoidal matter of Atriplex lindleyi Moq, *Int. J. Pharm. Pharm. Sci.*, 2014, **6**, 187–196.

23 S. Y. Ryu, C.-K. Lee, J. W. Ahn, S. H. Lee and O. P. Zee, Antiviral activity of triterpenoid derivatives, *Arch. Pharmacal Res.*, 1993, **16**, 339–342, DOI: **10.1007/BF02977528**.

24 K. Annan, R. Dickson, G. Komlaga, N. Jackson and G. Sam, Acaricidal effect of an isolate from Hoslundia opposita vahl against Amblyomma variegatum (Acari: Ixodidae), *Pharmacogn. Res.*, 2011, **3**, 185, DOI: **10.4103/0974-8490.85004**.

25 S. Faizi, H. Siddiqi, A. Naz, S. Bano and S. Lubna, Specific deuteration in patuletin and related flavonoids via keto-enol tautomerism: solvent- and temperature-dependent ^{1}H NMR Studies, *Helv. Chim. Acta*, 2010, **93**, 466–481, DOI: **10.1002/hlca.200900249**.

26 F. Li, Y. Han, X. Wu, X. Cao, Z. Cao, Y. Sun, M. Wang and H. Xiao, Gut microbiota-derived resveratrol metabolites, dihydroresveratrol and lunularin, significantly contribute

to the biological activities of resveratrol, *Front. Nutr.*, 2022, **9**, 912591, DOI: **10.3389/fnut.2022.912591**.

27 Z.-Q. Lu, P.-H. Fan, M. Ji and H.-X. Lou, Terpenoids and bisbibenzyls from Chinese liverworts *Conocephalum conicum* and *Dumortiera hirsuta*, *J. Asian Nat. Prod. Res.*, 2006, **8**(1–2), 187–192, DOI: **10.1080/1028602042000325537**.

28 R. S. Mali, K. N. Babu and P. G. Jagtap, Expedient syntheses of naturally occurring (±)-3-benzylphthalides and (±)-3-aryl-8-hydroxy-3,4-dihydroisocoumarins: structure revision of the (±)-3-benzylphthalide isolated from *Frullania falciloba*, *J. Chem. Soc., Perkin Trans. 1*, 2001, (22), 3017, DOI: **10.1039/B106268A**.

29 I. Komala, T. Ito, F. Nagashima, Y. Yagi and Y. Asakawa, Cytotoxic bibenzyls, and germacrane- and pinguisane-type sesquiterpenoids from Indonesian, Tahitian and Japanese liverworts, *Nat. Prod. Commun.*, 2011, **6**, 1934578X1100600, DOI: **10.1177/1934578X110060030**.

30 C.-M. Liu, R.-L. Zhu, R.-H. Liu, H.-L. Li, L. Shan, X.-K. Xu and W.-D. Zhang, cis-Clerodane diterpenoids from the liverwort *Gottschelia schizopleura* and their cytotoxic activity, *Planta Med.*, 2009, **75**, 1597–1601, DOI: **10.1055/s-0029-1185837**.

31 Y. Li, R. Zhu, J. Zhang, X. Wu, T. Shen, J. Zhou, Y. Qiao, Y. Gao and H. Lou, Clerodane diterpenoids from the Chinese liverwort *Jamesoniella autumnalis* and their anti-inflammatory activity, *Phytochemistry*, 2018, **154**, 85–93, DOI: **10.1016/j.phytochem.2018.06.013**.

32 T. H. Duong, N. K. V. Nguyen, T. Aree, N. T. Q. Trang, N. T. N. Thao, N. H. Tri, N. H. Nguyen and P. N. K. Tuyen, A new 3-benzylphthalide from the moss *Erythrodontium julaceum*, *Chem. Biodiversity*, 2003, e202301013, DOI: **10.1002/cbdv.202301013**.

33 F. Nagashima, M. Suzuki, S. Takaoka and Y. Asakawa, Sesqui- and diterpenoids from the Japanese liverwort *Jungermannia infusca*, *J. Nat. Prod.*, 2001, **64**, 1309–1317, DOI: **10.1021/np010223i**.

34 M. X. Lopes, L. M. V. Trevisan and V. d. S. Bolzani, Clerodane diterpenes from Aristolochia species, *Phytochemistry*, 1987, **26**, 2781–2784, DOI: **10.1016/S0031-9422(00)83590-6**.

35 M. D. Bomm, J. Zukerman-Schpector and L. M. X. Lopes, Rearranged (4→2)-abeo-clerodane and clerodane diterpenes from *Aristolochia chamissonis*, *Phytochemistry*, 1999, **50**, 455–461, DOI: **10.1016/S0031-9422(98)00583-4**.

36 C. Fazio, S. Passannanti, M. Pia Paternostro and F. Piozzi, Neo-clerodane diterpenoids from *Stachys rosea*, *Phytochemistry*, 1992, **31**, 3147–3149, DOI: **10.1016/0031-9422(92)83463-9**.

37 N. Nguyen, T. Duong, H. Truong Nguyen, Y. Vu, T. M. D. Tran, T. T. V. Ho, C. C. Mai, D. T. Mai, H. C. Nguyen, H. T. Le and D. D. Pham, New Halogenated flavonoids from *Adenosma bracteosum* and *Vitex negundo* and their α-glucosidase inhibition, *Chem. Biodiversity*, 2023, **20**, e202300390, DOI: **10.1002/cbdv.202300390**.

38 Y. Asakawa and A. Ludwiczuk, Chemical constituents of bryophytes: structures and biological activity, *J. Nat. Prod.*, 2018, **81**, 641–660, DOI: **10.1021/acs.jnatprod.6b01046**.

39 K. Dodo, A. Aoyama, T. Noguchi-Yachide, M. Makishima, H. Miyachi and Y. Hashimoto, Co-existence of α-glucosidase-inhibitory and liver X receptor-regulatory activities and their separation by structural development, *Bioorg. Med. Chem.*, 2008, **16**, 4272–4285, DOI: **10.1016/j.bmc.2008.02.078**.

40 C.-L. Tran, T.-B.-N. Dao, T.-N. Tran, *et al.*, Alpha-glucosidase inhibitory diterpenes from *Euphorbia antiquorum* growing in Vietnam, *Molecules*, 2021, **26**(8), 2257–2264, DOI: **10.3390/molecules26082257**.

41 J. Gasteiger and M. Marsili, Iterative partial equalization of orbital electronegativity—a rapid access to atomic charges, *Tetrahedron*, 1980, **36**, 3219–3228, DOI: **10.1016/0040-4020(80)80168-2**.

42 K. Stierand, P. Maaß and M. Rarey, Molecular complexes at a glance: automated generation of two-dimensional complex diagrams, *Bioinformatics*, 2006, **22**, 1710–1716, DOI: **10.1093/bioinformatics/btl150**.